Article

A One-Dimensional Blocking Index Becomes Two-Dimensional Using GIS Technology

Eli D. Ethridge [1], Bahtiyar Efe [2] and Anthony R. Lupo [1,*]

1   Atmospheric Science Program, School of Natural Resources, Missouri Climate Center, University of Missouri, Columbia, MO 65211, USA
2   Department of Meteorological Engineering, University of Samsun, 19 Mayis, Samsun 55420, Turkey
*   Correspondence: lupoa@missouri.edu; Tel.: +1-(573)-489-8457

Abstract: Many previous studies of the occurrence of blocking anticyclones, their characteristics, and dynamics have defined the onset longitude using the one-dimensional zonal index type criterion proposed by Lejenas and Okland. In addition to examining the blocking event itself, the onset longitude was determined to start at the nearest five degrees longitude using the National Centers for Environmental Prediction/National Center for Atmospheric Research Reanalyses that were used to identify the events. In this study, each blocking event in the University of Missouri Blocking Archive was re-examined to identify an onset latitude, and this information was added to the archive. The events were then plotted and displayed on a map of the Northern or Southern Hemisphere using Geographic Information System (GIS) software housed at the University of Missouri as different colored and sized dots according to block intensity and duration, respectively. This allowed for a comparison of blocking events in the archive above to studies that used a two-dimensional index. Then the common onset regions were divided by phase of the El Nino and Southern Oscillation (ENSO), and the typical onset of intense and persistent blocking events could be examined. The results found a favorable comparison between the onset regions identified here and those found in previous studies that used a two-dimensional blocking index. Additionally, there was variability identified in the onset regions of blocking in both hemispheres by ENSO phase, including the location of more intense and persistent events.

1. Introduction

In the previously published work by this laboratory, the blocking climatologies in [1–4] used the Lejenas–Okland Index [5] as their base criterion for identifying blocking events. This is a one-dimensional index that identifies the occurrence of blocking at a certain longitude. In [1], the longitude at which the blocking event was first identified was counted as the location for the event. As blocking events are quasi-stationary, the location of the occurrence of blocking over the lifetime of the event will not be far upstream or downstream of the onset location.

The work of [6] reviews three types of commonly used blocking indexes, which are zonal type, as proposed by [5,7]; thresholding type, as proposed by [8,9]; and potential vorticity type, as proposed by [10,11]. They [6] found that each index generates similar climatologies in spite of the fact that each has positive and negative qualities. Additionally, each index may not identify the exact same feature as blocking, and each generates slightly different blocking frequencies. As stated in [4] recently, arguably the zonal index criterion is the most frequently used, whether in one-dimensional or two-dimensional format.

In [4], using the one-dimensional index, blocking was most frequent in general for the Northern Hemisphere (NH) over the Pacific Region from 150° E to 120° W and in the

Atlantic-Continental Region from about 40° W to 90° E, with a minimum in occurrence from 100° W to 70° W. In the Southern Hemisphere (SH), only the South Pacific and far eastern Indian Ocean experience regular blocking activity occurring from approximately 110° E to 100° W. This review examined blocking over 51 seasons (NH) from 1968 to 2018 and 50 seasons in the SH (1970–2019). Comparing the late 20th century [2] to the early 21st century [3], the NH showed more blocking events and that the Atlantic Continental Region expanded slightly eastward from 60° E to 90° E, while the Pacific Region was a little less active from 150° E to the dateline. The overall location of local maxima remained similar, and [3] maintained the two distributions were similar at $p = 0.10$. The same publication found that block intensity and duration were correlated at $p = 0.01$ over both periods. In the SH [3], the similarity in genesis regions for the late 20th century versus the early 21st century was similar at $p = 0.01$, but the relationship between intensity and duration was only significant for the early 21st century ($p = 0.05$).

In this brief work, the location of blocking genesis regions displayed from [1–4] in one dimension will be displayed in two dimensions using Geographic Information System (GIS) technology for both hemispheres. The years since [3,4] will be added as well as the year 1969 for the SH. These will be compared to other works that use a two-dimensional index, e.g., [7,12,13]. Additionally, the blocking genesis region data will be examined with respect to phases of El Nino and Southern Oscillation (ENSO), which has not been conducted by this research group in the past. Finally, GIS technology will be exploited in order to determine the genesis location for blocking events of different durations and intensities. Block intensity (BI) is a diagnostic developed by this research group [1], and it is proportional to the strength of the 500 hPa height gradients [3].

2. Data and Methods

2.1. Data

The data used in this study were provided through the National Centers for Environmental Prediction/National Center for Atmospheric Research (NCEP/NCAR) 500 hPa reanalyses height fields on a 2.5° by 2.5° latitude-longitude gridded dataset available at 6-h intervals [14,15]. The 1200 UTC data were used in the calculation of BI as defined by [2] since these data include the most observational data. This study also used the blocking data archived in [16], which contains a list of all blocking events and their characteristics (see [1,2]) since 1 July 1968 for the NH and 1 January 1969 for the SH. The period of study here ends 30 June 2022 for the NH and 31 December 2022 for the SH, for a total of 54 years for both hemispheres. The reanalyses [15] were used by [1,2], and the rationale for the onset and termination dates of blocking events is described in these studies. Additionally, the starting and ending dates of the dataset chosen here correspond to the seasonality defined in [1] or [2].

In order to facilitate comparisons to previous studies in this group, the blocking seasons (regions) follow the blocking year (geographic boundaries) established by [1,2]. In particular, the boreal (austral) summer, fall, winter, and spring in the NH (SH) are July–September (January–March), October–December (April–June), January–March (July–September), and April–June (October–December), respectively. In the NH and SH (see Figure 1), the Atlantic Region (ATL) is defined as 80° W to 40° E and 60° W to 30° E, respectively. The Pacific Region is defined as 140° E to 100° W and 130° E to 60° W for the NH and SH, respectively. In the NH, the Continental Region (CON) encompasses 100° W to 80° W and 40° E to 140° E, while in the SH, the Indian Ocean Region (IND) is defined as 30° E to 130° E.
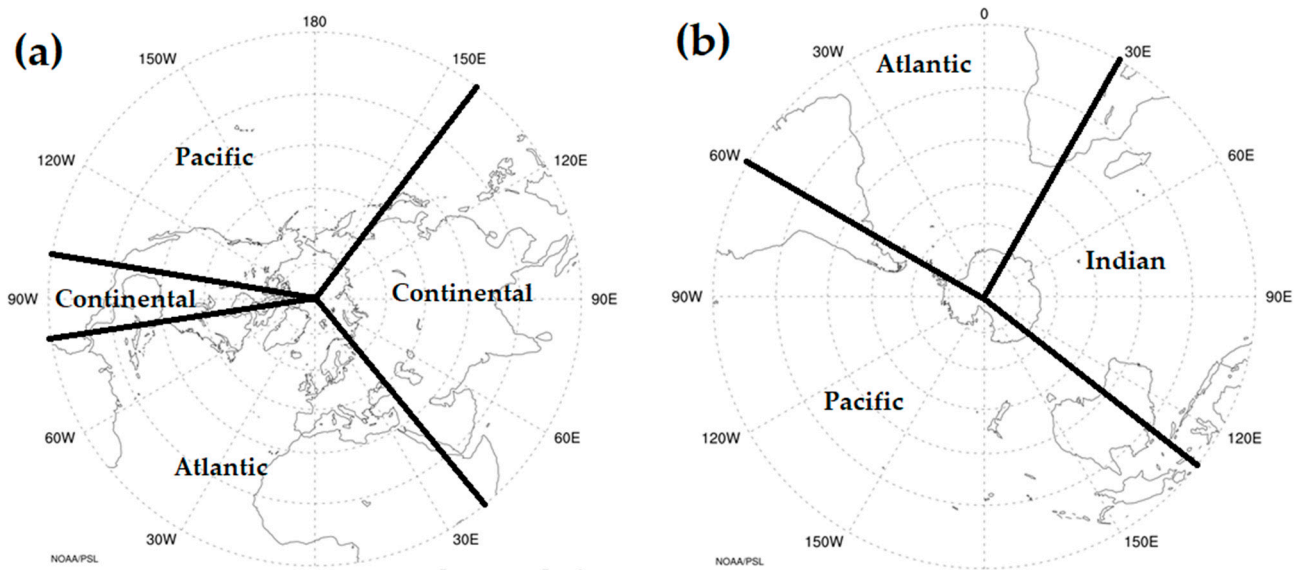
Figure 1. The study regions of the (**a**) NH and (**b**) SH. The lines denote the boundaries between the subregions described in the text.

2.2. Methods

The blocking criterion, duration, and BI used here were established by [1] and then automated and revised by [2] and the references therein. The definition of ENSO used in this study is described in [17] with references therein, and a short description is given here. The Japanese Meteorological Agency (JMA) ENSO index is available through the Center for Ocean and Atmospheric Prediction Studies (COAPS) from 1868 to the present [18]. The JMA classifies ENSO phases using SST within the bounded region of 4° S to 4° N, 150° W to 90° W, and defines the start of an ENSO year as 1 October and the end as 30 September of the following year; these years are shown in Table 1.

Table 1. List of ENSO years used here. The years below are taken from [18].

El Niño	Neutral	La Niña
1969	1968	1967
1972	1977–1981	1970–1971
1976	1983–1985	1973–1975
1982	1989–1990	1988
1986–1987	1992–1996	1998–1999
1991	2000–2001	2007
1997	2003–2005	2010
2002	2008	2017
2006	2011–2013	2020–2021
2009	2016	
2014–2015	2019	
2018		

The Pacific Decadal Oscillation (PDO) positive and negative modes are also found at COAPS. The most important reason for examining the PDO is its interaction with ENSO during certain phases, which creates either an enhanced or muted effect on temperatures and precipitation variability over the central USA, as found in many studies, e.g., [17,19–21]. The characteristics of the PDO are less pronounced than those of ENSO due to the fifty- to seventy-year length of the cycle [22,23]. The PDO positive phase is recognized as the period from 1977 to 1998, and the negative phases are recognized as the years 1947–1976 and 1999–2022.

3. Results

3.1. Comparison to the Previous Climatologies

An examination of the one-dimensional block genesis locations for the NH and SH by longitude, similar to that found in earlier studies from this group [1–4], is shown in Figure 2. In these previous works, the most common longitudes were determined subjectively. Here, common block genesis regions are defined by using the bin mean occurrence for each hemisphere. The bin mean occurrence is higher than the median block occurrence since the bin values are skewed toward higher occurrence frequencies. In the NH, the mean was 0.88 events per 10 degrees of longitude, and for the SH, it was 0.38 events. In the NH, the peak occurrences were determined as 150° E to 120° W and from 40° W to 60° E, which are slightly wider than the subjective locations identified in [3] but in agreement with a recent publication [24]. However, the peaks near 150° E, 180, and 150° W–130° W in the Pacific and near 0° and 30° E–60° E for the Atlantic–Eurasian Region were similar to those shown in [3]. For the SH, the locations between 110° E and 100° W were identified as the primary block genesis regions, which are also slightly wider than the subjective estimate given in [3]. However, the peaks near 160°–180° E and 130°–120° W are similar to those of previous studies. Additionally, the correlation for the duration to BI in the NH was 0.13, which is significant at $p = 0.01$, and in the SH it was 0.05, which is significant only at $p = 0.10$. This matches the results shown in [3,4].
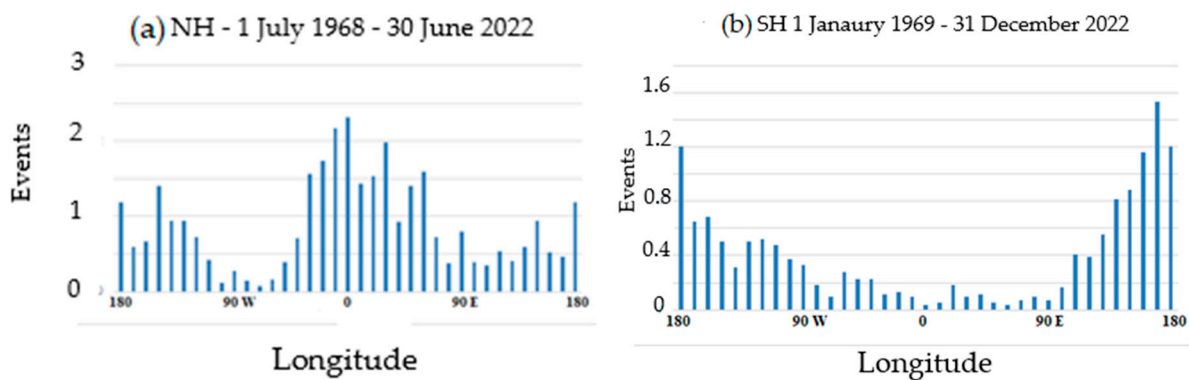

Figure 2. The location of blocking in the (**a**) NH and (**b**) SH binned using 10° latitude bins over 54 seasons in both hemispheres.

An examination of these distributions by ENSO phase is carried out by simply subtracting the mean block genesis regions for each phase of ENSO from the total sample. Thus, a positive (negative) number means more blocking at that longitude for the total (sub-) sample. For the NH, Figure 3a and Table 2 show that during Neu years there were fewer blocking events in the 0° to 40° E sector as well as over the west Pacific from 150° E to 180°. The primary and peak genesis regions were similar to the overall sample. During EN years (Figure 3c), there were fewer blocking events near the eastern coast of Asia (120° E to 140° E), but generally more events across the Pacific from 160° E to 90° W (except for 150° W to 140° W). This is consistent with the weaker Aleutian Low noted in [2] and references therein. In the Atlantic Region, there were fewer east Atlantic events (30° W to 10° W) and a greater number from 0° to 40° E. The result is a slightly wider blocking region for the Atlantic–Eurasian Sector. For LA years (Figure 3e), there were a greater number of blocking events from about 120° E to 140° W and fewer near the west coast of North America (130° W to 120° W); otherwise, the differences between the total sample and LN years were similar, except for some isolated longitudes. Testing the relationship between BI and duration shows that the correlation was 0.12, 0.20, and 0.10 for Neu, EN, and LA years, respectively. These values are significant at $p = 0.01$ for the former two and at $p = 0.05$ for the latter sample. Thus, the association was weakest in LA years and strongest in EN years.
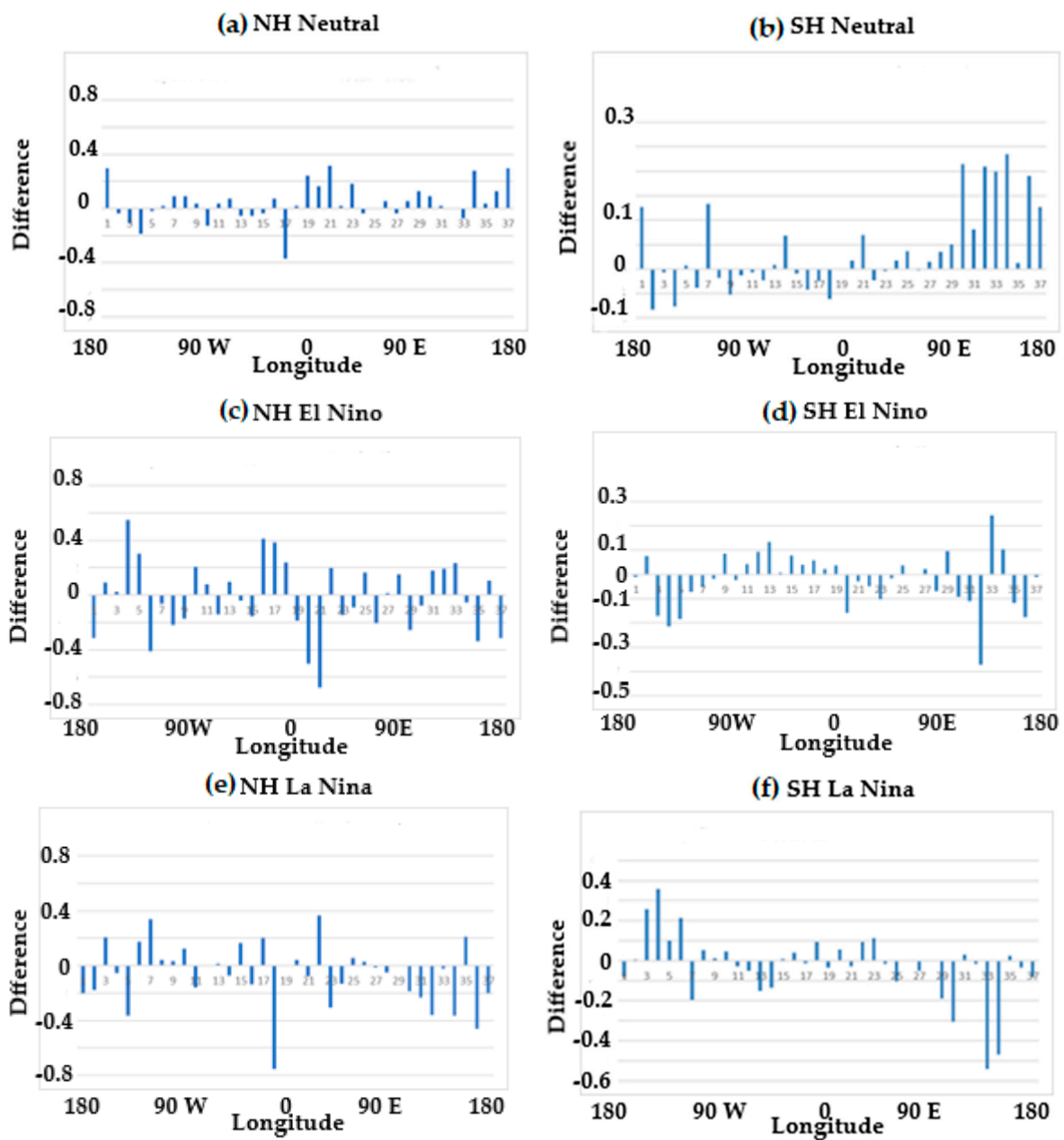
Figure 3. The difference between the mean occurrences of blocking by longitude for the total sample in the (**a**,**c**,**e**) NH and (**b**,**d**,**f**) SH by phase of ENSO, where (**a**,**b**), (**c**,**d**), and (**e**,**f**) are Neu, EN, and LA years, respectively.

In the SH, Figure 3b demonstrates that during neutral years there are fewer blocking events over the 110° E to 180° sector. The block genesis region during these years was identified as 130° E to 90° W, which is roughly 20° longitude east of the total sample distribution, but the peak is still around 160° E to 180°. For EN years (Figure 3d), there were more blocking events found over the central and eastern Pacific, especially for 160° W to 140° W, but otherwise the main and peak genesis regions were similar to the total sample. During LA years (Figure 3f), the block genesis region is shifted toward the west with respect to the total sample (100° E to 100° W—about 10° longitude), with the peak longitude as 140° E to 180°. These results for the whole 54-year sample agree with those found in [3] and references therein, which showed that during the negative phase of the Pacific Decadal Oscillation (PDO), LA blocking occurred further west in the Pacific. The negative PDO constitutes a larger fraction of the years here (32) versus the positive PDO (22).

Table 2. Character of NH (ATL/PAC/CON) and SH (ATL/PAC/IND) blocking events per year by region as a function of ENSO. The number of years in each category is shown in parenthesis. The units for occurrence is number of events, duration is days, and BI is a unitless number.

NH	Occurrence (Events)	Duration (Days)	Intensity
El Niño (14)	15.1/9.8/7.1	9.7/8.4/8.8	3.39/3.04/2.65
Neutal (27)	14.0/8.6/7.6	9.4/9.0/8.9	3.30/3.28/2.59
La Niña (13)	14.9/10.1/8.7	9.4/8.6/8.6	3.34/3.26/2.57
Total (54)	14.5/9.3/7.7	9.5/8.7/8.8	3.33/3.21/2.60
SH	**Occurrence (events)**	**Duration (days)**	**Intensity**
El Niño (14)	1.3/10.9/2.2	6.2/8.1/7.8	3.04/2.98/2.81
Neutral (26)	1.3/9.8/1.3	6.1/7.8/6.8	2.82/2.82/2.70
La Niña (14)	1.4/11.2/2.0	6.8/7.9/7.2	2.80/2.84/2.65
Total (54)	1.3/10.3/1.7	6.3/8.0/7.4	2.87/2.87/2.72

Testing the correlation between BI and duration revealed that the correlation was 0.07, 0.11, and −0.07 for Neu, EN, and LA, respectively. These values are significant at $p = 0.05$ for Neu and LA years and $p = 0.01$ for EN years. As with the NH, the association between BI and duration is strongest in EN years but weakest in LA years in general (Table 2). In fact, the correlation was opposite in the LA year, e.g., stronger blocks lasting fewer days. This accounts for the SH having a weaker association between BI and persistence in the total sample than the NH. In [3] for the SH, EN-year blocking events were the most persistent and strongest (Table 2). Thus, the strong correlation is not surprising. LN-year events were the least persistent and the weakest. However, [25] also demonstrated that the lesser persistence of SH blocking may be a function of the fact that the synoptic and large-scale interaction component of the flow is small compared to NH events. These scale interactions during LA years may be weak enough that the correlation between block duration and BI would not necessarily be positive. At least in the NH, [1] demonstrated a link between the vigor of upstream cyclogenesis, BI, and duration, and [25] (and references therein) demonstrated a strong synergistic synoptic and planetary-scale interaction at block onset. Thus, the stronger positive BI and persistence correlations are not surprising for the NH.

3.2. Results Using GIS

Displaying the blocking events by using their latitude and longitude at the first time they appear using GIS is shown in Figure 4. Given the resolution of the NCEP reanalyses, the onset location was given as the nearest gridpoint associated with the center of the blocking so that BI could be determined. Since each dot in Figure 4 represents the nearest point of onset for an individual event, a direct comparison to maps found in [12] or [13], which show a contoured percent of days that blocking was found at a particular gridpoint compared to the total number of days, may not be perfect. Additionally, the results shown in [12] cover the period 1950–2010.

However, in Figure 4a, it is apparent that there is a maximum in the eastern Pacific between 30° N and 40° N and 170° W and 130° W that corresponds to a similar feature shown in Figure 1 by [12]. A stronger maximum is found further poleward, centered near the Bering Strait, corresponding to those shown in both [12,13]. Thus, there is support for the methodology applied here. Additionally, note that thicker black circles represent points where more than one blocking event was identified as beginning at that location. In the Atlantic-Eurasian Region, Figure 4a shows agreement with [12,13] in terms of longitudinal extent, but the axis of the maximum latitude is found further south (approximately 35° N–50° N). This likely reflects the tendency of blocking events to have an onset at a more equatorward latitude (here) and for the center to migrate poleward throughout the lifecycle [12,13].
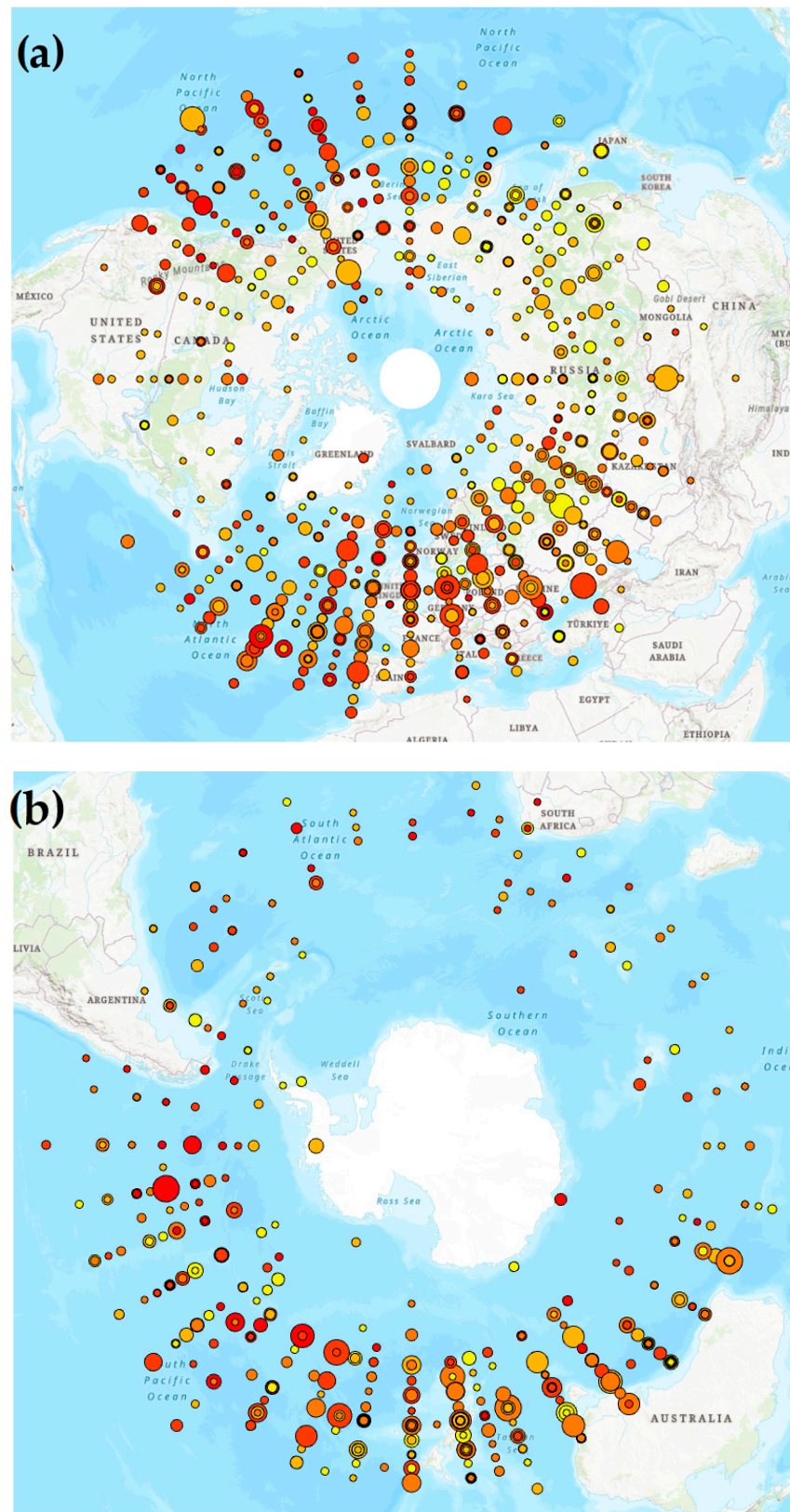
Figure 4. The GIS map for (**a**) NH and (**b**) SH blocking. The size of the marker corresponds to the duration of the blocking events, and the color from yellow to red corresponds to BI up to 2.0 (yellow), 2.0–3.0 (light orange), 3.0–4.0 (orange), 4.0–5.0 (red), and 5.0 and greater (deep red). The circles for duration are sized from least persistent (5 to 10 days) to most persistent (25 days or more).

One reason for comparing the results found here to [12] is that they used the BI diagnostic first published in [1] and then automated in [2]. In [12], the strongest blocking events were found in the East Pacific, while the most persistent were found near the Bering Strait and along the equatorward edge of the equatorward maximum identified above. Most of the deep red colors here in the Pacific are east of the dateline. It is more difficult to gauge correspondence between the larger dots here and the longer durations in [12] over the Pacific. In the Atlantic, the strongest events listed in [12] were located over the northeast Atlantic and northwest Europe, while the most persistent were found equatorward of Greenland and east of the Urals near central Asia. In Figure 4a, the strongest events appear over the northeast Atlantic and western Europe. Comparing duration may be more difficult due to the difference in variables displayed. Overall, however, there is good agreement between block onsets and BI here, as well as block locations and BI in [12].

In the SH, this work shows strong agreement with the work of [26] in that the Pacific Region from Australia to South America is the most prominent location for blocking. Sinclair [26] shows that the maximum region for blocking occurs poleward of about 35° S, which is consistent with the results found here. No other work of which the authors are aware uses a similar measure of intensity to BI in the SH. The most intense blocks occur in the East Pacific, with a few over the West Atlantic Region, as in [3]. The longest-lived blocking events are located closer to the dateline.

3.3. Interannual Variability Using GIS

The interannual variability using the GIS maps shows that for NH Neu years (Figure 5a), there were fewer overlapping occurrences west of 150° E and from 0° to 40° E. In Figure 5a, it is that clear there are fewer large markers and fewer with orange color in the west Pacific. Thus, it is clear that not only are there fewer events in west Pacific NEU years, but they have a shorter duration and a weaker BI. A comparison to Table 2 demonstrates that blocking in the eastern Pacific is of comparable duration and strength for the total sample and Neu years.

The occurrence of fewer blocking events over East Asia and the eastern Atlantic is also evident in Figure 5c for EN years. In fact, for these years, the East Asia region showed nearly as few events as can be found in North America. However, where blocking does occur more frequently, these events are as strong and intense as those occurring during the Neu years. In Figure 3e, fewer blocking events during LN years in the east Pacific near North America are also clear in Figure 5e. However, in Figure 5e, these events are weaker and less persistent. In fact, for these years, Figure 5e does not show the equatorward east Pacific maximum evident in the other phases and the total sample. This information could not be as easily displayed using previous analyses.

An examination of Figure 5b and comparison to Figures 3b and 4b shows that during SH Neu years, there were more blocking events found near Australia and the east Indian Ocean sector, and these events were found across the Pacific to South America, similar to the total sample. The strongest events are east Pacific events, but persistent events are found across the Pacific, confirming the results of [3,4].

In Figure 3d,f, the bar graphs implied that the East Pacific experienced more events during EN years, while during LN years, blocking occurrences were more confined west of the dateline and over eastern Australia. These results also agree with those found in [3,4] and in the works of [27–29]. Figure 5d implies that stronger blocks occur east of the dateline (3.18 units versus 2.88 units), and these are more persistent (8.7 versus 8.0 days) in EN years, but Figure 5f shows west Pacific blocking is weaker in BI (2.80 versus 3.08), but more persistent (7.9 versus 7.3 days) in LN years. This also corroborates the negative correlation found for BI and duration found only in SH LN years for blocking. Additionally, what has not been shown previously is that more persistent events onset at a more equatorward latitude for LN years (Figure 5f) than during other years.
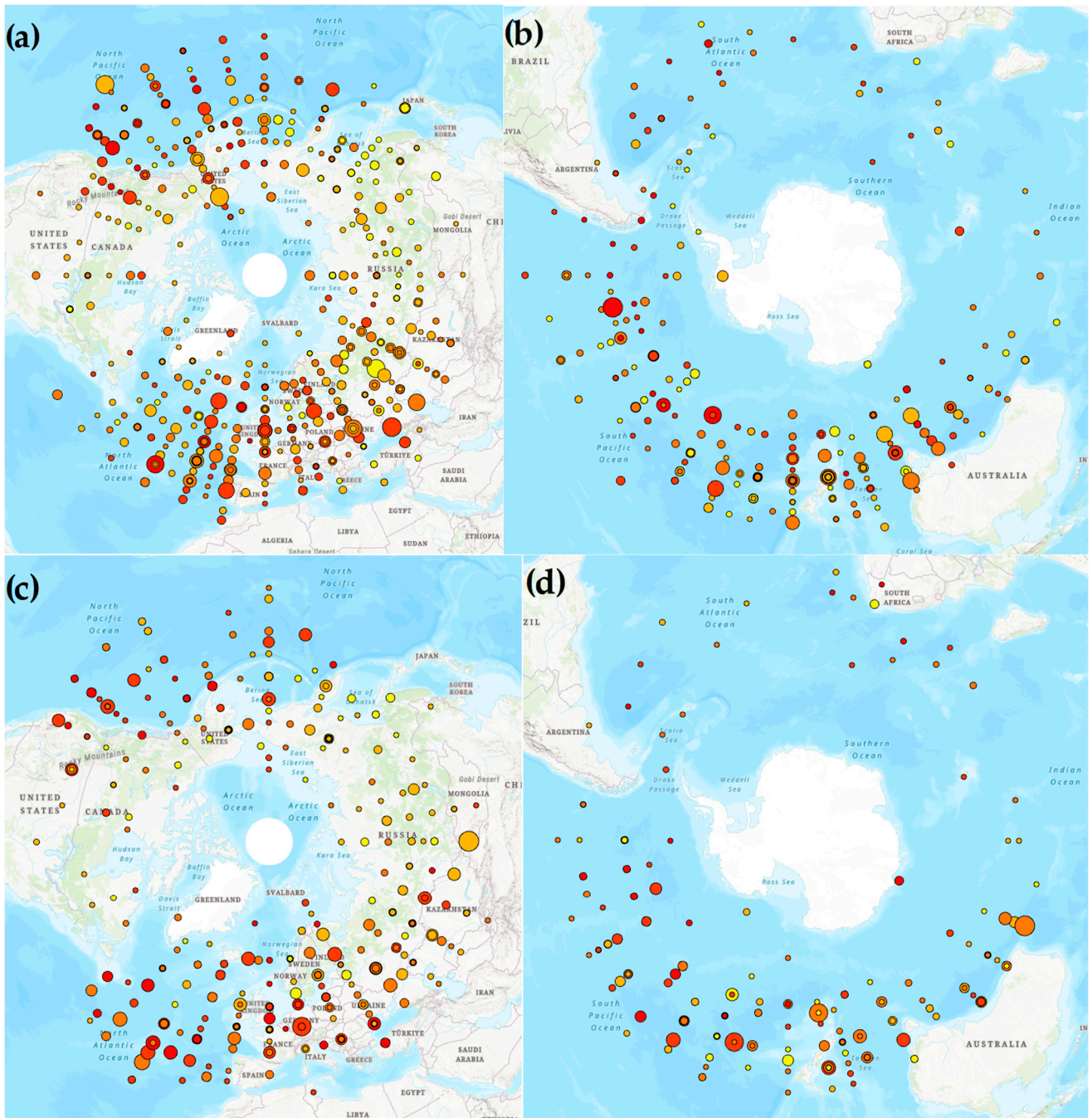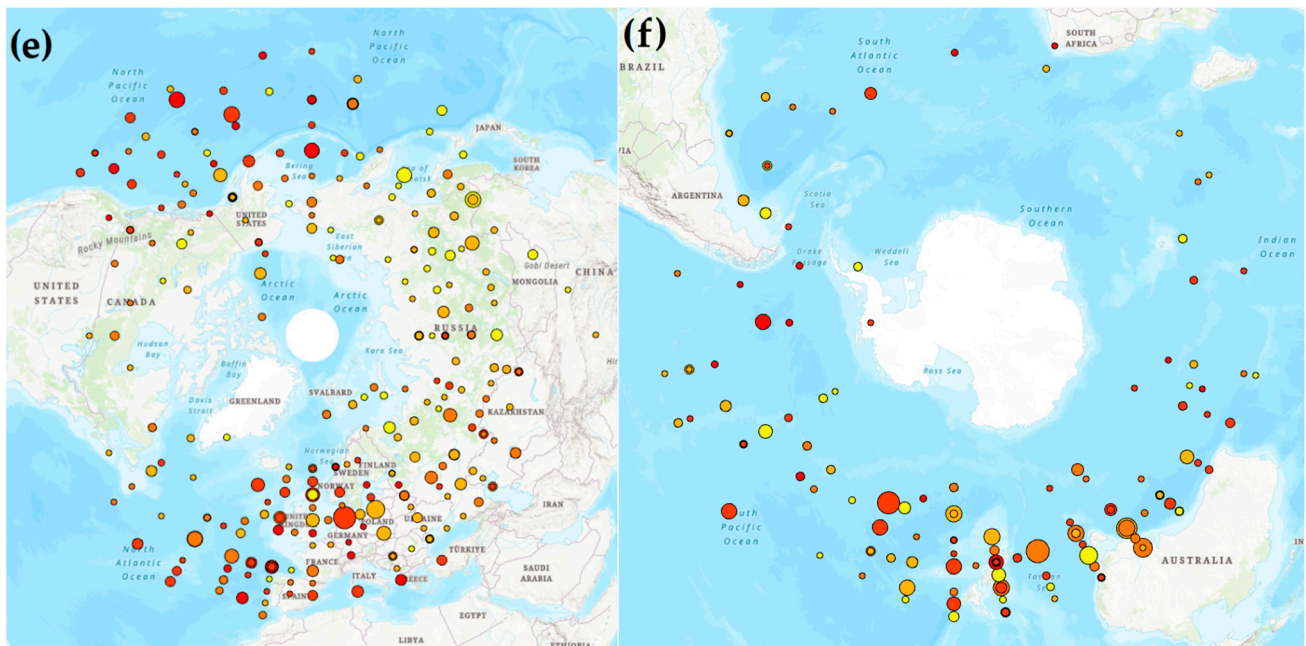
Figure 5. *Cont.*

Figure 5. The GIS map for (**a**,**c**,**e**) NH and (**b**,**d**,**f**) SH blocking, where (**a**,**b**), (**c**,**d**), and (**e**,**f**) are for Neu, EN, and LA years, respectively. The size of the marker corresponds to the duration of the blocking events, and the color from yellow to red corresponds to BI from 1.0 to 5.0 units and greater in increments of one unit. The circles for duration are sized from least persistent (5 to 10 days) to most persistent (25 days or more).

4. Discussion

The one-dimensional index used to study the location of block genesis was compared with previous climatologies from this group, and the block genesis regions were similar to the previous studies. Then, the results were broken down by ENSO phase. These results showed that there were some differences between typical block genesis regions during EN years versus LN years in the NH and SH. For example, during EN years, there were fewer events over east Asia and the west Pacific and more events east of 180° longitude. During the LN years, there were more events in East Asia through about 140° W and fewer near the west coast of North America. In the SH, there were generally fewer blocking events in the east Pacific and further west in LN years than in EN years.

However, when expanding these results to two dimensions, it was found that the general location of blocking was consistent with other studies that used two-dimensional indexes. It was also noted that the location of the stronger blocking events in the NH using the two-dimensional results matched those of [12], who also used the BI proposed by [1] and [2]. Further, it was found that in the NH Pacific region there were two maxima for peak block occurrence, one in the Bering Sea and the other in the southeast Pacific, similar to that identified in [12].

Further, the two-dimensional results presented here allowed for the identification of differences by ENSO phase. In the NH, there were fewer blocking events during LN years in the southeast Pacific, and these were weaker and less persistent. This would be consistent with a weaker storm track in that region, as shown by [30]. During EN years, the stronger and more poleward storm track identified for EN years in [31] corresponds to the more active blocking region found over 0°–40° E compared to LN years. Additionally, Figure 5 showed these events were more persistent and stronger in EN years compared to LN years. These results would have been more difficult to discern without the two-dimensional GIS plotting.

In the SH, it was clear that EN year blocking in the East Pacific was more frequent, persistent, and stronger than during LN years. Blocking during LN years was confined to the

east coast of Australia and the western Pacific region. These blocking events occurred about 10 degrees latitude equatorward of those occurring during EN years, which is consistent with [32]. Additionally, these results corroborate the negative correlation between BI and duration found for SH LN years. It is likely that synoptic and planetary scale interactions during the block lifecycles in the SH found by [25] explain this correlation. Finally, the two-dimensional SH results generally show agreement with the results of [28,29], as well as those of [32], which also show a weaker storm track in the eastern Pacific during LN years.

5. Conclusions

In this study, the one-dimensional objective blocking criterion of [5] used by previous studies from this research group [1–4] was expanded to two dimensions by identifying the latitude of all blocking events recorded in the blocking archive found at [16]. Then the latitude/longitude coordinates of each blocking event were plotted on a map using GIS technology to mark these events by color for intensity and marker size for the duration. This was conducted for the entire 54-year period from July 1968 to June 2022 for the NH and January 1969 to December 2022 for the SH.

The following new results were obtained from this study: First, this study identified the primary blocking regions in both the NH and SH using an objective criterion (the mean occurrence in ten-degree longitude bins). This criterion identified primary blocking regions in the Atlantic and Pacific regions that were slightly broader than those identified subjectively in previous publications.

Using the one-dimensional index from the previous studies of this group, the primary locations for blocking in the NH and SH were more frequent in the east (west) Pacific for EN (LN) years. Additionally, the correlation between block intensity (BI) and duration was strongest in both hemispheres during EN years, and weakest in LN years. In fact, for the SH, the correlation was negative, and it was proposed here that this was due to the interaction between blocking and the upstream cycle events or storm tracks.

When including the latitude for the onset of blocking, the results plotted here using GIS maps to represent BI and duration show that the two-dimensional block formation regions match well with studies that used a two-dimensional block index to identify primary NH blocking regions. In the Pacific, there were two block formation regions identified, one in the eastern Pacific and one west of the North American continent. These are where more intense blocks form in the Pacific. The other region is in the Bering Strait. In the Atlantic, the results found here were consistent with those shown in recent studies, except a little further equatorward in this study. The difference is likely due to the fact that here, block onset is identified, whereas, in the comparative studies, they identified all blocking days.

In the SH, there is good agreement with previous studies using a two-dimensional blocking index. Additionally, it was found that the strongest blocking events were located within the east Pacific and west Atlantic, while the most persistent blocking events occur between Australia and the western to central Pacific.

When interannual variability was examined, the following results were obtained: In the NH, where blocking events were less frequent using the one-dimensional index, they were also less frequent using the two-dimensional maps here. Where these events were less frequent, they were also weaker and less persistent. In the SH, the same relationships were generally found, and during LN years, blocking was slightly equatorward to those in EN years. Lastly, the negative correlation for SH blocking events between BI and persistence in LN years is demonstrated by the greater frequency of deep red and smaller markers on the GIS maps.

Finally, given the success of using the GIS mapping tools with the one-dimensional blocking index favored by this research group, the interannual variability of blocking character by season and region will be studied in the future. Additionally, this methodology can be applied to model projections in order to determine the future blocking character that includes BI.

References

1. Lupo, A.R.; Smith, P.J. Climatological features of blocking anticyclones in the Northern Hemisphere. *Tellus* **1995**, *47*, 439–456. [CrossRef]
2. Wiedenmann, J.M.; Lupo, A.R.; Mokhov, I.I.; Tikhonova, E.A. The climatology of blocking anticyclones for the Northern and Southern Hemisphere: Block intensity as a diagnostic. *J. Clim.* **2002**, *15*, 3459–3474. [CrossRef]
3. Lupo, A.R.; Jensen, A.D.; Mokhov, I.I.; Timazhev, A.V.; Eichler, T.E.; Efe, B. Changes in global blocking character during the most recent decades. *Atmosphere* **2019**, *10*, 92. [CrossRef]
4. Lupo, A.R. Atmospheric Blocking Events: A Review. *Ann. New York Acad. Sci. Spec. Issue Year Clim. Sci. Res.* **2021**, *1504*, 5–24. [CrossRef] [PubMed]
5. Lejenäs, H.; Økland, H. Characteristics of Northern Hemisphere blocking as determined from a long time series of observational data. *Tellus* **1983**, *35*, 350–362. [CrossRef]
6. Pinheiro, M.C.; Ullrich, P.A.; Grotjahn, R. Atmospheric blocking and intercomparison of objective detection methods: Flow field characteristics. *Clim. Dyn.* **2019**, *53*, 4189–4216. [CrossRef]
7. Tibaldi, S.; Molteni, F. On the operational predictability of blocking. *Tellus* **1990**, *42*, 343–365.
8. Elliott, R.D.; Smith, T.B. A study of the effects of large-blocking highs on the general circulation in the Northern Hemisphere westerlies. *J. Meteorol.* **1949**, *6*, 67–85. [CrossRef]
9. Dole, R.M.; Gordon, N.D. Persistent anomalies of the extratropical Northern Hemisphere wintertime circulation: Geographical distribution and regional persistence characteristics. *Mon. Weather Rev.* **1983**, *111*, 1567–1586. [CrossRef]
10. Pelly, J.L.; Hoskins, B.J. A new perspective on blocking. *J. Atmos. Sci.* **2003**, *60*, 743–755. [CrossRef]
11. Schwierz, C.; Croci-Maspoli, M.; Davies, H.C. Perspicacious indicators of atmospheric blocking. *Geophys. Res. Lett.* **2004**, L06125. [CrossRef]
12. Davini, P.; Cagnazzo, C.; Gualdi, S.; Navarra, A. A bidimensional diagnostics, variability, and trends of Northern Hemisphere blocking. *J. Clim.* **2012**, *25*, 6496–6509. [CrossRef]
13. Woollings, T.; Barriopedro Cepero, D.; Methven, J.; Son, S.-W.; Harvey, B.; Martius, O.; Sillmann, J.; Lupo, A.R.; Seneviratne, S. Blocking and it's response to climate change. *Curr. Clim. Change Rep.* **2018**, *4*, 287–300. [CrossRef] [PubMed]
14. Kalnay, E.; Kanamitsu, M.; Kistler, R.; Collins, W.; Deaven, D.; Gandin, L.; Iredell, M.; Saha, S.; White, G.; Woollen, J.; et al. The NCEP/NCAR 40-year reanalysis project. *Bull. Am. Meteorol. Soc.* **1996**, *77*, 437–471. [CrossRef]
15. NCEP/NCAR Reanalyses Project. Available online: http://www.esrl.noaa.gov/psd/data/reanalysis/reanalysis.shtml (accessed on 24 October 2022).
16. University of Missouri Blocking Archive. Available online: http://weather.missouri.edu/gcc (accessed on 24 October 2022).
17. Newberry, R.G.; Lupo, A.R.; Jensen, A.D.; Rodriges-Zalipynis, R.A. An analysis of the spring-to-summer transition in the West Central Plains for application to long range forecasting. *Atmos. Clim. Sci.* **2016**, *6*, 375–393. [CrossRef]
18. Center for Ocean and Atmosphere Prediction Studies. Available online: http://www.coaps.fsu.edu (accessed on 11 May 2017).
19. Bove, M.C.; Elsner, J.B.; Landsea, C.W.; Niu, X.; O'Brien, J.J. Effects of El Niño on U.S. Landfalling Hurricanes, Revisited. *Bull. Amer. Meteor. Soc.* **1998**, *79*, 2477–2482. [CrossRef]
20. Hu, Z.Z.; Huang, B. Interferential Impact of ENSO and PDO on Dry and Wet Conditions in the U.S. Great Plains. *J. Clim.* **2009**, *19*, 5500–5518. [CrossRef]
21. Birk, K.; Lupo, A.R.; Guinan, P.E.; Barbieri, C.E. The interannual variability of midwestern temperatures and precipitation as related to the ENSO and PDO. *Atmofera* **2010**, *23*, 95–128.

22. Mantua, N.J.; Hare, S.R.; Zhang, Y.; Wallace, J.M.; Francis, R.C. A Pacific Interdecadal Climate Oscillation with Impacts on Salmon Production. *Bull. Amer. Meteor. Soc.* **1997**, *78*, 1069–1079. [CrossRef]
23. Minobe, S. A 50–70-Year Climatic Oscillation over the North Pacific and North America. *Geophys. Res. Lett.* **1997**, *24*, 683–686. [CrossRef]
24. Yuchechen, A.E.; Lakkis, S.G.; Canziani, P.O. The Southern Hemisphere blocking index revisited. *Atmosphere* **2022**, *13*, 1343. [CrossRef]
25. Burkhardt, J.P.; Lupo, A.R. The planetary and synoptic-scale interactions in a Southeast Pacific blocking episode using PV diagnostics. *J. Atmos. Sci.* **2005**, *62*, 1901–1916. [CrossRef]
26. Sinclair, M.R. A climatology of anticyclones and blocking for the Southern Hemisphere. *Mon. Weather Rev.* **1996**, *124*, 245–263. [CrossRef]
27. Marques, R.F.C.; Rao, V.B. Interannual variations of blockings in the Southern Hemisphere and their energetics. *J. Geophys. Res.* **2000**, *105*, 4625–4636. [CrossRef]
28. Oliveira, F.N.M.; Carvalhoc, L.M.V.; Ambrizzi, T. A new climatology for southern hemisphere blockings in the winter and the combined effect of ENSO and SAM phases. *Int. J. Climatol.* **2014**, *34*, 1676–1692. [CrossRef]
29. O'Kane, T.J.; Monselesan, D.P.; Risbey, J.S. A Multiscale Reexamination of the Pacific–South American Pattern. *Mon. Weather Rev.* **2017**, *145*, 379–402. [CrossRef]
30. Eichler, T.; Higgins, W. Climatology and ENSO-Related Variability of North American Extratropical Cyclone Activity. *J. Clim.* **2004**, *19*, 2076–2093. [CrossRef]
31. Liao, C.; Xu, H.; Deng, J.; Zhang, L. Interannual Relationship between ENSO and Atlantic Storm Track in Spring Modulated by the Atlantic Multidecadal Oscillation. *Atmosphere* **2018**, *9*, 419. [CrossRef]
32. Solman, S.A.; Menendez, C.G. ENSO-Related Variability of the Southern Hemisphere Winter Storm Track over the Eastern Pacific–Atlantic Sector. *J. Atmos. Sci.* **2002**, *59*, 2128–2140. [CrossRef]